SCIENCE CHINA
Earth Sciences

• RESEARCH PAPER •

November 2014 Vol.57 No.11: 2702–2711
doi: 10.1007/s11430-014-4970-9

Detrital zircon U-Pb-He double dating: A method of quantifying long- and short-term exhumation rates in collisional orogens

Christina Yan WANG[1,2*], Ian H. CAMPBELL[2], Peter W. REINERS[3] & Charlotte M. ALLEN[2]

[1]*Key Laboratory of Mineralogy and Metallogeny, Guangzhou Institute of Geochemistry, Chinese Academy of Sciences, Guangzhou 510640, China;*
[2]*Research School of Earth Sciences, The Australian National University, Canberra, ACT 0200, Australia;*
[3]*Department of Geosciences, University of Arizona, Tucson, AZ 85721, USA*

Received October 11, 2013; accepted January 21, 2014; published online September 25, 2014

A U-Pb-He double-dating method is applied to detrital zircons with core-rim structure from the Ganges River in order to determine average short- and long-term exhumation rates for the Himalayas. Long-term rates are calculated from the U/Pb ages of metamorphic rims of the grains that formed during the Himalayan orogeny and their crystallization temperatures, which are calculated from the Ti-in-zircon thermometer. Short-term rates are calculated from (U-Th)/He ages of the grains with appropriate closure temperatures. The results show that short-term rates for the Himalayas, which range from 0.70 ± 0.09 to 2.67 ± 0.40 km/Myr and average 1.75 ± 0.59 (1σ) km/Myr, are higher and more varied than the long-term rates, which range from 0.84 ± 0.16 to 1.85 ± 0.35 km/Myr and average 1.26 ± 0.25 (1σ) km/Myr. The differences between the long-term and short-term rates can be attributed to continuous exhumation of the host rocks in different mechanisms in continental collision orogen. The U/Pb ages of 44.0 ± 3.7 to 18.3 ± 0.5 Ma for the zircon rims indicate a protracted episode of ~25 Myr for regional metamorphism of the host rocks at deeper crust, whereas the (U-Th)/He ages of 42.2 ± 1.8 to 1.3 ± 0.2 Ma for the zircon grains represent a protracted period of ~40 Myr for exposure of the host rocks to shallower crustal level. In particular, the oldest (U-Th)/He ages of the zircon grains are close to the oldest U/Pb ages for the rims, indicating that some parcels of the rocks that contain zircons were rapidly exhumed from deep to shallow levels in the stage of collisional orogeny. On the other hand, some parcels of the rocks may have been carried upwards by thrust faults in the post-collisional stage. The parcels could be carried upwards by the thrust faults that steepen as they near the surface, or by transient movement faults so that areas of rapid exhumation became areas of slow exhumation and visa versa on a time scale of a few Myr in order to maintain the continuous exhumation. In this regard, the Ganges River must be preferentially sampling areas that are currently undergoing above average rates of uplift.

zircon, U-Pb-He double-dating method, Himalayas, exhumation rate, collisional orogen

Citation: Wang C Y, Campbell I H, Reiners P W, et al. 2014. Detrital zircon U-Pb-He double dating: A method of quantifying long- and short-term exhumation rates in collisional orogens. Science China: Earth Sciences, 57: 2702−2711, doi: 10.1007/s11430-014-4970-9

Quantitative studies of exhumation rates place important constraints on landscape evolution and on hypotheses for the formation of mountain belts. Exhumation rates have traditionally been determined by dating minerals of known closure temperature in igneous or metamorphic rocks (e.g., Copeland et al., 1987), or by thermochronology of detrital minerals collected from rivers (e.g., Jain et al., 2000; Brewer et al., 2003). The advantage of the former is that multiple minerals, with different closure temperatures, can be dated

*Corresponding author (email: wang_yan@gig.ac.cn)

from the same rock allowing the exhumation history for the rock to be documented. A disadvantage is that regional coverage is time consuming and often difficult, especially in rugged terrains. Thermochronology of detrital minerals gives convenient regional coverage but existing techniques do not allow the measurement of short- and long-term exhumation rates on the same grain. Short- and long-term exhumation rates can be determined for a drainage system by dating detrital minerals with different closure temperatures, but there is no way of determining whether the minerals come from the same or different sources.

This study reports a U-Pb-He double-dating method in which short- and long-term exhumation rates can be determined on a single detrital zircon with core-rim structure. Our method provides three dates: a U/Pb date of the core that gives the crystallization age of the zircon, a U/Pb date of the rim that gives the crystallization age of zircons from metamorphic fluids during orogeny and a (U-Th)/He date of the bulk grain that gives its cooling age. The crystallization temperatures of the rims can be calculated from their Ti contents using the Ti-in-zircon thermometer of Watson and Harrison (2005). An appropriate closure depth is calculated by assuming an equilibrium thermal model for the exhuming crust, using the Age2Edot program 2.1 described in Reiners and Brandon (2006). Short- and long-term cooling and exhumation rates can be calculated from these data. We demonstrate the utility of this method by applying it to detrital zircons from the Ganges River to determine the average short- and long-term exhumation rate for the Himalayas.

1 Sampling and analytical method

Analyses were performed on a single sample collected from the bank of the Ganges River in 2003, 700 km up river from the Bangladesh border, near Kanpur (Figure 1). Detrital zircons were separated from sands using conventional magnetic and heavy liquid separation techniques.

An Excimer Laser Ablation Inductively Coupled Plasma Mass Spectrometry (ELA-ICP-MS, Agilent 7500) at the Research School of Earth Sciences, Australian National University was used to date the zircons by the U/Pb method. Unpolished whole zircons were mounted on double-sided adhesive tape and were simultaneously dated for U/Pb ages and analyzed for Ti by ELA-ICP-MS, using the rim-piercing method of Campbell et al. (2005). The 30-μm-wide laser holes were drilled through the top of grains to produce continuous 20 μm depth profiles of $^{206}Pb/^{238}U$ ratio from the rims of the grains towards their centers as shown in Figure 2. This procedure allows us to date rims as narrow as 5 μm that cannot be dated by other

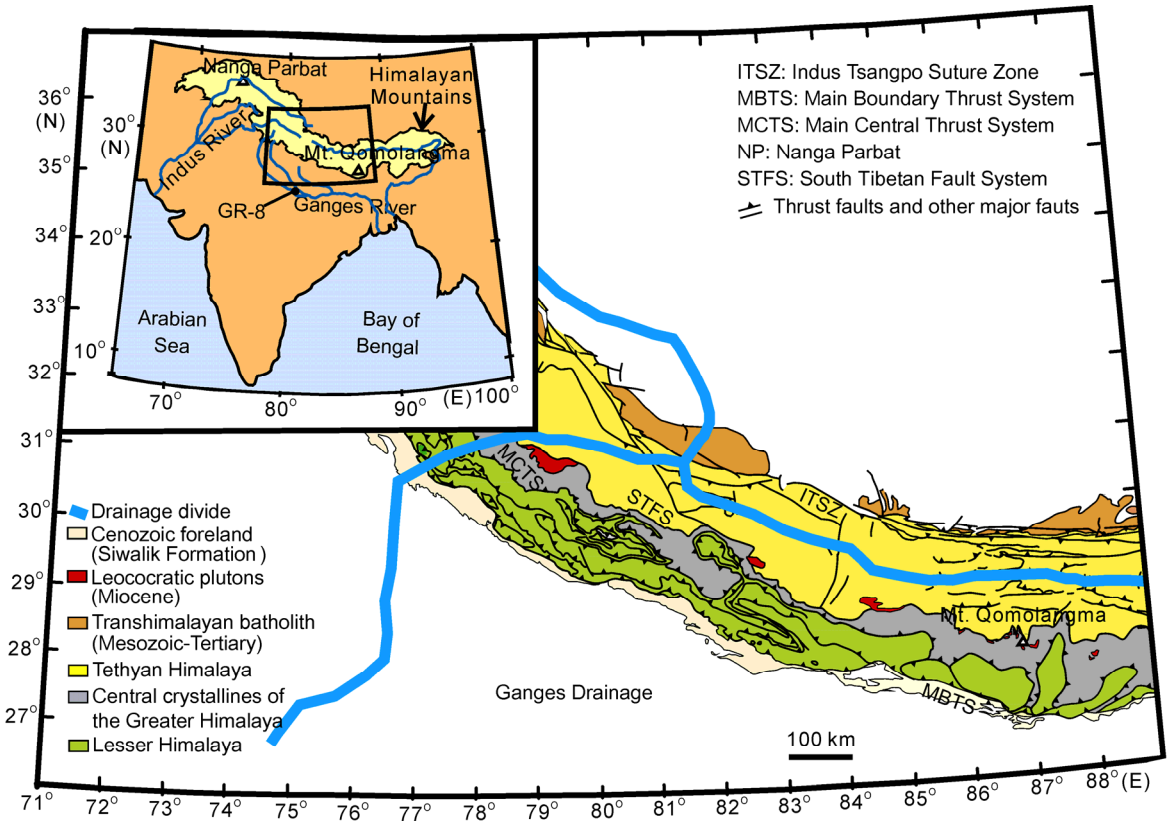

Figure 1 Geological sketch map of the Himalayan Mountains and Tibetan Plateau (simplified from Hodges, 2000) showing the outline of the Ganges River drainage basin. The insert shows the location of sample GR-8 used in this study.

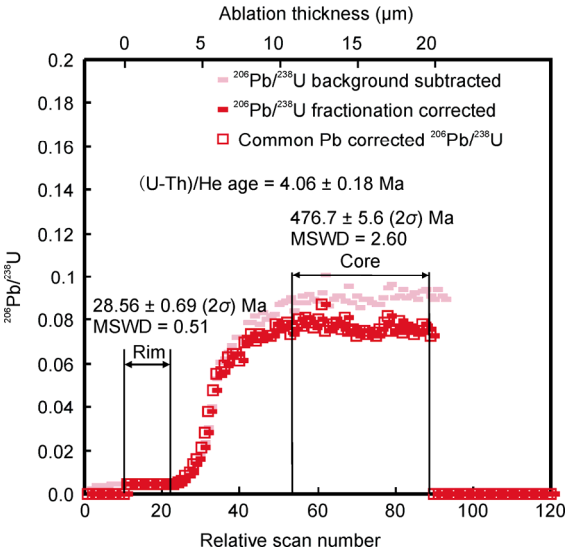

Figure 2 A continuous profile of ^{206}Pb/^{238}U ratios for an age-zoned grain (GR8-622) against relative scan number obtained by ELA-ICP-MS showing that both rim and core of the grain is datable to give precise U/Pb ages. Common Pb correction is based on the method by Compston et al. (1984).

methods. The integration time was 40 ms for three Pb isotopes, U and Th, and 10 ms for all other isotopes with a total mass sweep time of 0.385 s. Each ablation consumes a large amount of material that may include inclusions of minerals such as apatite or material that is age-zoned. The response time of the ablation cell in ANU lab, which we define as the time the signal takes to decay by a factor of 10, is ~2 s. This rapid response time allows us to edit out sections of the profile that are age-zoned or contain inclusions. Campbell et al. (2005) described the U/Pb dating method used in this study in greater detail.

Following U/Pb dating the zircons were removed from the tape and their (U-Th)/He ages were measured by standard procedures involving Nd-YAG laser heating and Parr bomb dissolution. The detailed (U-Th)/He dating method used in this study was described by Reiners (2005). Note that the laser-ablation process does not alter (U-Th)/He ages, as has been demonstrated by multiple single-grain replicates of zircons from the Fish Canyon Tuff and other standards (Rahl et al., 2003). Farley et al. (1996) demonstrated that (U-Th)/He ages typically require correction for the effects of alpha-ejection from crystals. The age-zoned zircons typically show systematic core-to-rim zonation of U and Th that can cause inaccuracy in alpha-ejection-corrected (U-Th)/He ages (Farley et al., 1996; Reiners et al., 2004; Hourigan et al., 2005). In most cases of this study, the rims have higher U and lower Th than the cores. Although in general this may cause a bias to younger ages in grains requiring alpha-ejection corrections, it is not likely to exceed ~10% to 15% (Hourigan et al., 2005) because most grains show core-to-rim concentration contrasts of less than a factor of ~2—3, and have opposing Th and U zonation patterns.

Corrected (U-Th)/He ages have been selected for all euhedral grains in this study. However, a few grains studied here show morphologies, indicating that no alpha-ejection corrections are required due to strong abrasion and rounding during transport. For these grains the raw ages have been used, which is appropriate if the high-U rims were abraded during the most recent cycle of transport and sedimentation. On the other hand, if the analyzed zircon was a recycled grain that was abraded during an earlier sedimentary cycle, using the uncorrected age may be inappropriate. The upper uncertainty for the rounded grains has been extended to the corrected age in recognition of this possibility.

To test the possibility that variable (U-Th)/He ages are due to strong variation in He retentivity among the zircons, we dated (U-Th)/He ages for ten detrital grains from two sandstones from the metamorphic aureole around the 433±3 Ma Cooma Granite, south of Canberra, Australia (Williams, 2001). The samples were taken from the biotite and migmatic grade zones. The results are listed in Table 1. Figure 3 shows (U-Th)/He ages are plotted against eU (eU = U + 0.235Th). (U-Th)/He ages of seven grains with eU < 865 ppm agree within error of the mean age of 321±14 Ma, whereas metamict grains with higher eU appear to have lost He, consistent with observations from other zircons with a range of accumulated radiation damage (e.g., Reiners, 2005). The potential for increased He diffusivity from high eU and very old zircons is not relevant here because of the extremely young (U-Th)/He ages of the zircons in this study. However, the above data do indicate that grains with very low eU may have slightly younger ages, consistent with slightly higher He diffusivity in grains with low radiation damage, similar to observations in apatite (Shuster et al., 2006), and consistent with decreasing anisotropy of He diffusion (Farley, 2007) with increasing radiation damage.

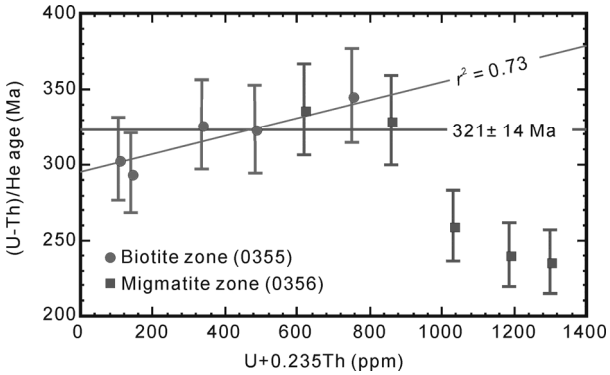

Figure 3 A plot of (U-Th)/He age against eU (where eU = U + 0.235Th) showing the relationship of (U-Th)/He ages and He retentivity among the zircons.

2 Results

A total of 140 zircons were analyzed by U/Pb dating method, and 22 of them were selected for (U-Th)/He dating: 18 age-zoned zircons with rims that are wide enough (>5 μm) to be dated for both U/Pb core and rim ages, and four grains without age zonation to be dated for bulk-grain U/Pb ages and (U-Th)/He ages.

2.1 Zircon grains with age zonation

The U/Pb ages and crystallization temperatures of 18 grains with age zonation are listed in Table 2 and (U-Th)/He ages are listed in Table 3. The U/Pb rim ages of the age-zoned grains range from 18.3 ± 0.5 to 44.0 ± 3.7 Ma and temperatures vary between 577 ± 9°C and 721 ± 5°C. The U/Pb core ages of the zoned zircons vary from 176 ± 16 to 2811 ± 8 Ma and temperatures vary from 603 ± 18°C to 756 ± 23°C. Their (U-Th)/He ages vary between 1.3 ± 0.2 and 42.2 ± 1.8 Ma, with most grains having (U-Th)/He ages much younger than the U/Pb rim ages (Figure 4).

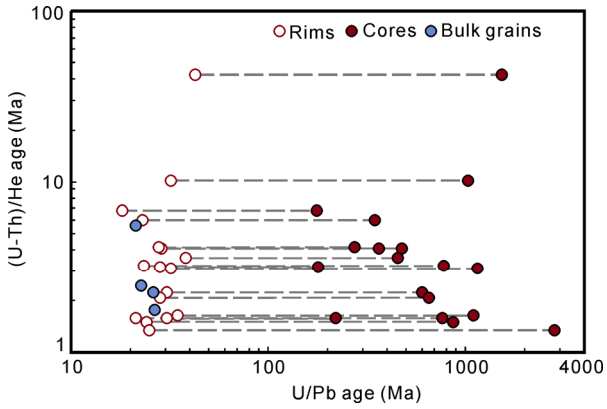

Figure 4 A plot of core and rim U/Pb ages versus (U-Th)/He ages showing relatively constant rim U/Pb ages against variable core U/Pb ages.

2.2 Zircon grains without age zonation

Four grains without age zonation have U/Pb ages ranging from 21.3 ± 0.5 to 26.7 ± 0.9 Ma (Table 1). Their (U-Th)/He ages range from 1.8 ± 0.1 to 5.6 ± 0.2 Ma (Table 2), much younger than their U/Pb ages (Figure 4). Their crystallization temperatures vary between 595 ± 6°C and 699 ± 5°C (Table 2).

3 Long- and short-term cooling and exhumation rates

Long-term rates are calculated from the U/Pb ages of the zircon rims and crystallization temperature of the zircon obtained from the Ti-in-zircon thermometer, which assumes that zircon growth occurs in equilibrium with rutile from a zircon-saturated fluid (Watson and Harrison, 2005). This assumption is reasonable for the zircon rims because rutile-bearing meta-sediments are the dominant rock type in the high-grade metamorphic rocks of the Himalayas. If rutile is absent during zircon growth the calculated temperatures will be low by up to 60°C (Watson and Harrison, 2005), which will not affect the conclusions of this study.

Short-term rates are calculated from the (U-Th)/He ages of the grains, and calculation of the appropriate closure depth assuming an equilibrium thermal model for the exhuming crust, using the Age2Edot program 2.1 described in Reiners and Brandon (2006). This model accounts for the significant increase in the geothermal gradient of the upper crust produced by heat advection during rapid exhumation. The upper and lower boundary conditions were set at 10°C at the surface and 700°C at 35 km, based on peak *P-T* conditions for the high-grade Greater Himalayan Crystalline Complex (after Yin, 2006). No such correction was applied to the long-term exhumation rate because the correction is small and less than the uncertainty in the parameters used for the lower boundary condition.

Table 1 (U-Th)/He ages of 10 detrital zircons from two sandstone samples from the metamorphic aureole around the 433 ± 3 Ma Cooma Granite, Australia

Sample No.	U (ppm)	Th (ppm)	Th/U	^{4}He (nmol/g)	Mass (μg)	M_{war} (μm)	Raw age (Ma)	± (1σ)	Error (%)	Corrected age (Ma)	f_{ap} error (Ma)	f_{ap} error (%)
ANU03-055-04	313	101	0.32	497.6	6.79	67.0	268	6.01	2.24	326	7.3	2.2
ANU03-055-07	92.3	64.8	0.70	152.8	13.4	75.0	258	5.51	2.14	303	6.5	2.1
ANU03-055-14	455	132	0.29	747.4	14.8	84.8	278	6.04	2.17	323	7.0	2.2
ANU03-055-22	131	53	0.40	189.9	6.80	66.5	241	5.29	2.19	294	6.4	2.2
ANU03-055-26	654	436	0.67	1212.9	10.5	71.5	290	5.94	2.05	345	7.1	2.0
ANU03-056-05	844	84	0.10	1059.2	1.53	31.3	223	4.90	2.20	329	7.2	2.2
ANU03-056-09	1229	321	0.26	1276.4	3.31	43.3	179	3.81	2.13	235	5.0	2.1
ANU03-056-13	576	188	0.33	821.7	3.49	32.3	241	5.08	2.11	336	7.1	2.1
ANU03-056-16	996	167	0.17	1111.1	4.17	41.0	196	4.22	2.15	259	5.6	2.2
ANU03-056-22	1097	391	0.36	1226.9	6.97	45.8	188	3.99	2.12	240	5.1	2.1

Table 2 U/Pb ages and crystallization temperatures based on the Ti-in-zircon thermometer for detrital zircon grains from the Ganges River

Sample No.	Age zonation	Core							Rim						
		Age[a] (Ma)	±(2σ)	Th[b] (ppm)	U[b] (ppm)	Th/U	Ti[b] (ppm)	Temp[c] (°C)	Age[a] (Ma)	±(2σ)	Th[b] (ppm)	U[b] (ppm)	Th/U	Ti[b] (ppm)	Temp[c] (°C)
GR8-513	yes	1037	12	118	307	0.38	2.72	638 ± 19	31.93	1.59	25.8	854	0.03	1.92	614 ± 8
GR8-518	yes	1533	51	165	213	0.77	4.21	670 ± 20	43.97	3.70	8.80	686	0.01	2.65	636 ± 19
GR8-525	yes	763	13	176	118	1.49	3.45	655 ± 20	21.27	0.82	4.77	448	0.01	2.25	625 ± 10
GR8-605	yes	176	16	24	2701	0.01	2.97	644 ± 19	18.32	0.49	64.6	4189	0.02	3.01	645 ± 3
GR8-607	yes	345	9	4	632	0.01	3.08	647 ± 19	23.24	1.48	10.9	1450	0.01	3.54	657 ± 10
GR8-608	yes	180	10	35	3735	0.01	11.6	754 ± 23	28.10	0.83	41.3	6116	0.01	7.93	721 ± 5
GR8-610	yes	1152	42	256	279	0.92	9.31	730 ± 22	32.13	1.88	3.54	1366	0.00	1.08	577 ± 9
GR8-622	yes	476	6	55	3909	0.01	2.97	644 ± 19	28.56	0.69	10.8	3590	0.00	1.86	612 ± 8
GR8-626	yes	458	8	35	1016	0.03	3.52	657 ± 20	38.37	1.97	11.4	2379	0.00	1.79	609 ± 11
GR8-631	yes	867	19	96	102	0.94	4.34	672 ± 20	24.20	1.72	4.93	710	0.01	1.80	610 ± 9
GR8-637	yes	362	4	13	4049	0.00	2.13	621 ± 19	28.92	2.25	16.0	3053	0.01	1.49	597 ± 16
GR8-639	yes	1100	8	462	1890	0.24	7.07	711 ± 21	34.80	1.39	3.07	748	0.00	1.29	588 ± 9
GR8-657	yes	2811	8	213	452	0.47	7.71	719 ± 22	25.02	1.12	3.92	839	0.00	1.42	594 ± 8
GR8-659	yes	772	12	92	122	0.75	8.40	726 ± 22	23.53	1.59	8.39	1013	0.01	2.04	618 ± 10
GR8-665	yes	276	8	29	941	0.03	3.48	656 ± 20	27.66	1.26	15.8	2319	0.01	1.79	610 ± 9
GR8-667	yes	600	24	81	154	0.53	11.8	756 ± 23	30.87	1.39	143	2759	0.05	5.11	685 ± 6
GR8-675	yes	657	7	191	905	0.21	2.76	639 ± 19	28.24	0.96	14.6	823	0.02	6.10	699 ± 5
Gr8-684	yes	220	9	38	1277	0.03	1.62	603 ± 18	30.42	0.68	4.08	659	0.01	2.50	632 ± 13
GR8-625	no	21.27	0.53	27.5	8330	0.00	2.91	643 ± 5							
GR8-632	no	22.77	0.77	34.0	1994	0.02	3.51	657 ± 6							
GR8-660	no	26.70	0.90	17.1	2312	0.01	1.44	595 ± 6							
GR8-679	no	26.29	1.09	7.98	905	0.01	6.06	699 ± 5							

a) Common ^{206}Pb-uncorrected ^{206}Pb/^{238}U ages are used for grains younger than 900 Ma, whereas common ^{206}Pb-uncorrected ^{207}Pb/^{206}Pb ages are used for those older than 900 Ma; b) trace elemental concentrations and their detection limits in zircons are based on the method of Longerich et al. (1996), using NBS NIST 610 as the standard. The NIST 610 values are based on Pearce et al. (1997). The absolute concentration of elements in zircons was determined by ratioing to SiO_2 and assuming a stoichiometric concentration of 32.77 wt.% of SiO_2 in zircons; c) crystallization temperatures were calculated from the Ti-in-zircon thermometer (Watson and Harrison, 2005). The temperature should be regarded as a minimum temperature if the zircon growth is not in equilibrium with rutile in the zircon-saturated melt (Watson and Harrison, 1983).

Calculated long- and short-term cooling and exhumation rates are summarized in Table 4. The long-term cooling rates vary between 15.9 ± 1.8 and 35.2 ± 3.6°C/Myr, averaging 24.0 °C/Myr, and the short-term rates between 15 ± 2 and 120 ± 12°C/Myr, averaging 62 °C/Myr. No cooling rate has been calculated for GR8-518, which has a U/Pb rim age of 44.0 ± 3.7 Ma and a He age of 42.2 ± 1.8 Ma. These two ages agree within error. The long-term exhumation rates range from 0.84 ± 0.16 to 1.85 ± 0.35 km/Myr, averaging 1.26 ± 0.25 (1σ) km/Myr, whereas short-term rates show a wider range and vary between a minimum of 0.70 ± 0.09 km/Myr and a maximum of 2.67 ± 0.40 km/Myr, averaging 1.75 ± 0.59 km/Myr (Table 4). Four zircons have short-term rates that are lower than their long-term rates whereas the remaining 17 grains have short-term rates that are up to 2.7 times higher than their long-term rates. Clearly the short-term rates are more variable and generally higher than the long-term rates (Figure 5).

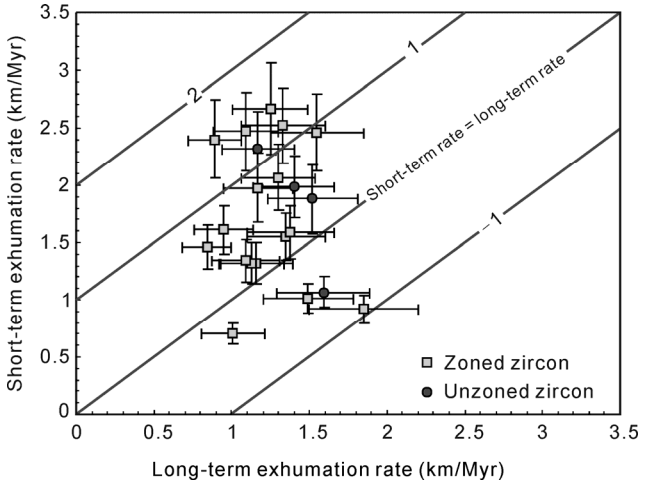

Figure 5 A plot of long-term exhumation rates versus short-term exhumation rates showing that the short-term rates are more variable and generally higher than the long-term rates.

Table 3 (U-Th)/He ages for detrital zircon grains from the Ganges River[a)]

Sample No.	Morphology	Age zonation	U (ppm)	Th (ppm)	Th/U	Ft	^{4}He (nmol/g)	Mass (μg)	M_{war} (μm)	Raw age (Ma)	± (1σ)	Error (%)	Corrected age (Ma)	± (1σ)	Error (%)	Age selected	Negative uncertainty	Positive uncertainty
GR8-513	rounded	yes	607	94.4	0.16	0.77	34.1	3.57	47.3	10.1	0.22	2.17	13.0	0.28	2.17	10.1*	0.22	2.9
GR8-518	rounded	yes	871	461	0.53	0.65	224	1.03	28.3	42.2	0.92	2.18	65.0	1.41	2.18	42.2 *	0.92	22.8
GR8-525	euhedral	yes	206	134	0.65	0.78	1.56	4.01	47.5	1.22	0.03	2.56	1.57	0.04	2.56	1.57	0.04	0.04
GR8-605	very euhedral	yes	3924	108	0.03	0.78	112	7.42	46.0	5.28	0.12	2.21	6.75	0.15	2.21	6.75	0.15	0.15
GR8-607	mostly euhedral	yes	569	53.1	0.09	0.81	15.0	6.31	55.3	4.78	0.11	2.21	5.91	0.13	2.21	5.91	0.13	0.13
GR8-608	irregular/rounded	yes	7871	173	0.02	0.69	133	1.90	35.0	3.12	0.07	2.16	4.55	0.10	2.16	3.12*	0.07	1.42
GR8-610	euhedral	yes	1024	198	0.19	0.73	13.1	2.37	38.3	2.28	0.05	2.21	3.10	0.07	2.21	3.10	0.07	0.07
GR8-622	euhedral	yes	2882	92.4	0.03	0.80	50.9	8.07	51.5	3.25	0.07	2.18	4.06	0.09	2.18	4.06	0.09	0.09
GR8-626	euhedral	yes	1556	77.9	0.05	0.76	23.0	4.47	40.5	2.71	0.06	2.19	3.58	0.08	2.19	3.58	0.08	0.08
GR8-631	mostly euhedral	yes	411	145	0.35	0.80	2.88	5.80	53.5	1.20	0.03	2.46	1.50	0.04	2.46	1.50	0.04	0.04
GR8-637	euhedral	yes	5706	62.2	0.01	0.79	98.5	8.51	45.3	3.20	0.08	2.35	4.04	0.10	2.35	4.04	0.10	0.10
GR8-639	rounded	yes	914	223	0.24	0.80	8.51	6.36	50.5	1.63	0.06	3.41	2.05	0.07	3.41	1.63*	0.06	0.42
GR8-657	very rounded	yes	390	82.4	0.21	0.78	2.96	4.12	48.5	1.34	0.06	4.28	1.72	0.07	4.28	1.34*	0.06	0.38
GR8-659	mostly euhedral	yes	414	70.5	0.17	0.74	5.48	4.31	36.5	2.36	0.09	3.77	3.18	0.12	3.77	3.18	0.12	0.12
GR8-665	mostly euhedral	yes	811	86.3	0.11	0.77	14.4	3.70	46.8	3.21	0.08	2.50	4.14	0.10	2.50	4.14	0.10	0.10
GR8-667	mostly euhedral	yes	515	115	0.22	0.69	4.48	2.01	32.0	1.53	0.07	4.53	2.22	0.10	4.53	2.22	0.10	0.10
GR8-675	rounded	yes	804	143	0.18	0.74	9.31	2.11	41.0	2.06	0.06	3.04	2.79	0.08	3.04	2.06*	0.06	0.73
GR8-684	mostly rounded	yes	1121	156	0.14	0.69	9.86	1.96	31.3	1.58	0.05	2.98	2.29	0.07	2.98	1.58*	0.05	0.07
GR8-625	euhedral	no	6407	214	0.03	0.81	156	9.00	52.0	4.49	0.10	2.19	5.56	0.12	2.19	5.56	0.12	0.12
GR8-632	very euhedral	no	1174	51.8	0.04	0.75	11.7	4.06	39.8	1.83	0.09	4.89	2.43	0.12	4.89	2.43	0.12	0.12
GR8-660	rounded	no	992	361	0.36	0.75	10.3	2.51	43.3	1.77	0.05	2.90	2.37	0.07	2.90	1.77*	0.05	0.59
GR8-679	mostly euhedral	no	706	53.9	0.08	0.74	6.35	4.13	36.3	1.64	0.04	2.59	2.21	0.06	2.59	2.21	0.06	0.06

a) The ages marked with * are raw ages without alpha-ejection correction (see the text for explanation).

Table 4 Cooling and exhumation rates calculated from U/Pb and (U-Th)/He ages for detrital zircons from the Ganges River

Sample No.	Age zonation	U-Pb method				(U-Th)/He method				ΔE[a)] (km/Myr)
		T (°C)	Rim age (Ma)	Long-term cooling rate (°C/Myr)	Long-term exhumation rate (km/Myr)	T_c (°C)	Age (Ma)	Short-term cooling rate (°C/Myr)	Short-term exhumation rate (km/Myr)	
GR8-605	yes	645 ± 3	18.3 ± 0.5	35.2 ± 3.6	1.85 ± 0.35	191	6.75 ± 0.30	24 ± 2	0.92 ± 0.12	–0.93
GR8-625	no	643 ± 5	21.3 ± 0.5	30.2 ± 3.1	1.59 ± 0.30	193	5.56 ± 0.24	29 ± 3	1.07 ± 0.14	–0.52
GR8-607	yes	657 ± 10	23.2 ± 1.5	28.3 ± 3.3	1.49 ± 0.29	192	5.91 ± 0.26	27 ± 3	1.01 ± 0.13	–0.48
GR8-513	yes	614 ± 8	31.9 ± 1.6	19.2 ± 2.2	1.01 ± 0.20	186	10.0 ± 0.4	15 ± 2	0.70 ± 0.09	–0.31
GR8-665	yes	610 ± 9	27.7 ± 1.3	22.0 ± 2.5	1.16 ± 0.23	196	4.14 ± 0.21	37 ± 3	1.32 ± 0.18	0.16
GR8-622	yes	612 ± 8	28.6 ± 0.7	21.4 ± 2.3	1.13 ± 0.21	196	4.06 ± 0.18	36 ± 3	1.32 ± 0.18	0.19
GR8-608	yes	721 ± 5	28.1 ± 0.8	25.7 ± 2.4	1.35 ± 0.25	199	3.12 ± 0.14	52 ± 3	1.55 ± 0.21	0.20
GR8-659	yes	618 ± 10	23.5 ± 1.6	26.3 ± 3.2	1.38 ± 0.28	199	3.18 ± 0.24	51 ± 5	1.59 ± 0.23	0.21
GR8-637	yes	597 ± 16	28.9 ± 2.3	20.6 ± 2.7	1.09 ± 0.22	196	4.04 ± 0.19	40 ± 3	1.34 ± 0.18	0.25
GR8-632	no	657 ± 6	22.8 ± 0.8	28.8 ± 2.9	1.52 ± 0.29	202	2.43 ± 0.24	66 ± 7	1.88 ± 0.30	0.36
GR8-679	no	699 ± 5	26.3 ± 1.1	26.6 ± 2.7	1.40 ± 0.26	202	2.21 ± 0.11	73 ± 5	1.99 ± 0.27	0.59
GR8-626	yes	609 ± 11	38.4 ± 2.0	15.9 ± 1.8	0.84 ± 0.16	198	3.58 ± 0.16	45 ± 5.5	1.46 ± 0.19	0.62
GR8-610	yes	577 ± 9	32.1 ± 1.9	18.0 ± 2.2	0.95 ± 0.19	199	3.10 ± 0.14	52 ± 4	1.61 ± 0.21	0.66
GR8-675	yes	699 ± 5	28.2 ± 1.0	24.8 ± 2.4	1.30 ± 0.24	203	2.06 ± 0.13	80 ± 6	2.07 ± 0.29	0.77
GR8-667	yes	685 ± 6	30.9 ± 1.4	22.2 ± 2.3	1.17 ± 0.22	202	2.22 ± 0.20	73 ± 8	1.98 ± 0.30	0.81
GR8-525	yes	625 ± 10	21.3 ± 0.8	29.4 ± 3.2	1.55 ± 0.30	206	1.57 ± 0.08	98 ± 7	2.46 ± 0.33	0.91
GR8-660	no	595 ± 6	26.7 ± 0.9	22.3 ± 2.5	1.17 ± 0.23	205	1.77 ± 0.10	69 ± 5	2.32 ± 0.32	1.15
GR8-631	yes	610 ± 9	24.2 ± 1.7	25.2 ± 3.1	1.33 ± 0.27	207	1.50 ± 0.07	110 ± 8	2.52 ± 0.33	1.19
Gr8-684	yes	632 ± 13	30.4 ± 0.7	20.8 ± 2.1	1.09 ± 0.21	206	1.58 ± 0.09	105 ± 8	2.47 ± 0.34	1.38
GR8-657	yes	594 ± 8	25.0 ± 1.1	23.7 ± 2.7	1.25 ± 0.24	208	1.34 ± 0.11	120 ± 12	2.67 ± 0.40	1.42
GR8-639	yes	588 ± 9	34.8 ± 1.4	16.9 ± 1.9	0.89 ± 0.17	206	1.63 ± 0.11	101 ± 8	2.40 ± 0.34	1.51
GR8-518	yes	636 ± 19	44.0 ± 3.7				42.2 ± 1.8			

a) ΔE is the difference between the short and long term exhumation rate. We have assumed errors of ± 3% in the temperature calculated from measured Ti content, ± 1.5% in the calibration of zircon thermometer, with an additional uncertainty of 10% in case the activity of TiO_2 is not one, ±15% in the geothermal gradient, and ± 2 to 8% in the U-Pb age based on counting statistics for the individual zircon dates, which give a total error of ±4 to 8% in the estimation of cooling rate and ± 16 to 18% in the estimation of the exhumation rate from the U-Pb ages. An error of 5 % is assigned to the calculated closure temperature, ±12.5% to the exhumation rate calculation and ± 9 to 13% in the (U-Th)/He ages of individual zircon based on counting statistics, which give a total error of ±10 to 14% for the cooling rates and ± 13 to 18% for the (U-Th)/He age based exhumation rates.

4 Significance of U/Pb core and rim age of zircon and (U-Th)/He age of zircon

4.1 Old cores of zircons

The U/Pb core ages of the age-zoned zircons in this study are older than the Himalayan orogeny and date the pre-Himalayan igneous bodies from which the original zircons were ultimately derived, normally an earlier orogenic event (Campbell et al., 2005). Their variability indicates that their source, during the most recent erosion cycle, was meta-sedimentary rock. Although the U/Pb ages of the pre-Himalayan cores are not used in the exhumation or cooling rate calculations, the recognition of old cores is critical to the interpretation for long-term exhumation rates. Conventional U/Pb-He double-dating method of detrital zircons (e.g. Campbell et al., 2005), without narrow rims, cannot be used to obtain long-term exhumation rates because of the possibility that zircon crystallized from a magma that cooled at a higher crustal level and was not in thermal equilibrium with its surroundings. If the degree of partial melting is high enough to produce abundant new zircons the magma may move from its source to a highly level in the crust, which if unrecognized, will lead to an overestimation of the exhumation rate.

The four grains without age zonation have U/Pb ages younger than the onset age of the Indian-Eurasia collision (~50 Ma, Besse et al., 1984; Beck et al., 1998; Yin and Harrison, 2000 and references therein; Zhu et al., 2005). Their (U-Th)/He ages are much younger than their U/Pb ages so they are primary first-cycle plutonic zircons formed during the Himalayan orogeny (Campbell et al., 2005). For the reason given above the cooling and exhumation rates derived from these grains should be treated with caution. However, both their short- and long-term exhumation rates are similar to the rimed grains (Figure 5) suggesting that even if they have been transported in melts they have not traveled far.

4.2 U/Pb ages of zircon rims and (U-Th)/He ages of zircons

The U/Pb ages for the narrow rims of zircon grains date the overgrowth of metamorphic zircon that occurred during the Himalayan orogeny. This is because most of the rims have low Th concentration and low Th/U ratios (Table 2), indicating the crystallization from metamorphic fluids at subsolidus conditions rather than anatectic melts at suprasolidus conditions (Zheng, 2009; Li et al., 2013). Therefore, the rims would crystallize *in situ* on pre-existing detrital zircon grains in meta-sediments that underwent metamorphic dehydration.

The rims of zircon grains have U/Pb ages ranging from 18.3 ± 0.5 to 44.0 ± 3.7 Ma. The range of the U/Pb ages indicates a protracted episode as long as ~25 Myr for regional metamorphism of the host rocks at deep crust, i.e., a process from continental collision to postcollisional reworking. The upper U/Pb age limit yielded by the zircon rims in this study is consistent with the U/Pb ages of 44±3 Ma for the rim of zircon with a Permian core, a garnet–omphacite Sm-Nd isochron age of 49 ± 6 Ma, a phengite Rb-Sr isochron age of 43 ± 1 Ma for the Kaghan eclogite in Pakistan (Tonarini et al., 1993) as well as a U/Pb age of 50 Ma for overgrown quartz-bearing rims and a U/Pb age of 46 Ma for coesite-bearing rim (Kaneko et al., 2003; Parrish et al., 2006). The long episode of 40–50 Myr is common for high-pressure (HP) to ultrahigh-pressure (UHP) metamorphism in continent-continent collisional orogens such as the Dabei-Sulu in China and the Western Gneiss Region in Norway, whereas the short episode of 5–10 Myr is prominent in arc-continent collisional orogens such as the Himalayas and Alps (Zheng, 2012; Zheng et al., 2013). As the HP to UHP eclogite-facies metamorphism in the Himalayas was considered to have lasted for 5—10 Myr (after Zheng, 2012), the long episode of ~25 Myr recorded in the rims of the zircons in this study may indicate the zircon overgrowth during the prolonged overprinting of amphibolite-facies metamorphism in the Himalayas.

The (U-Th)/He ages of the zircon grains range from 1.3 ± 0.2 to 42.2 ± 1.8 Ma, indicating a protracted period of ~40 Myr for the exposure of the host rocks to shallow crustal level. Note that the oldest (U-Th)/He ages of the zircon grains are close to the oldest U/Pb ages of the rims, indicating that the exposure of the rocks at deep crust could have occurred in the late episode of the continental collision during the Himalaya orogeny.

5 Long- and short-term exhumation rates

5.1 Comparison with previous studies

Our short-term exhumation rates for the Himalayas are consistent with previous estimates when all data are corrected for advective heat transfer. Burbank et al. (2003) reported apatite-fission-track derived exhumation rates of 2.25–3.75 km/Myr for ten samples from the Greater Himalaya and Tibetan Plateau, collected from a tributary to the Ganges River. Jain et al. (2000) measured apatite and zircon fission track ages for the Central Crystallines of the Greater Himalayas from the Sutiej River in the Indus basin that yield exhumation rates of 2.8–1.5 km/Myr and 3.1–2.2 km/Myr, respectively. Samples from the Lesser Himalayas from the same region gave apatite fission track exhumation rates between 1.25 and 0.8 km/Myr. Finally, direct determination of short-term erosion rates in the Upper Ganges catchment by ^{10}Be and ^{26}Al measurements of quartz from river sands gives erosion rates of 2.7 ± 0.3 km/Myr for the Greater Himalaya, 1.2 ± 0.1 km/Myr for the Tibetan Plateau, and 0.8 ± 0.3 km/Myr for the Lesser Himalaya (Vance et al.,

2003), similar to the range of our short-term exhumation rates (0.70 ± 0.09 to 2.67 ± 0.40 km/Myr).

5.2 Possible controls on the differences between short- and long-term exhumation rates

The results in this study indicate that the short-term exhumation rates are variable and that most of zircons have short-term exhumation rates higher than their long-term rates, however, four zircons have higher long-term exhumation rates than short-term rates (Table 4 and Figure 5). There are a number of possible explanations for the difference between the short- and long-term exhumation rates. First the difference could be due to the onset of the late Cenozoic glaciation in the Northern Hemisphere or to recent intensification of the Asian monsoon (Clift et al., 2008 and reference therein). Although these are contributing factors they are unlikely to dominate. A remarkable log-linear correlation between relief and denudation over three orders of magnitude in several studies shows that relief is the dominant factor controlling denudation (Ahnert, 1970; Vance et al., 2003 and references therein). Glaciers and monsoons, in the absence of relief, are ineffective agents of erosion.

A second explanation for the difference between the average short- and long-term exhumation rates is that rivers provide a biased sample by preferentially sampling areas that are currently undergoing anomalously high rates of crustal uplift and erosion, and the areas of rapid uplift and exhumation change from time to time (France-Lanord et al., 1993; Stewart et al., 2008). This conclusion is consistent with a study of detrital zircons from the Indus River, which showed that ~75% of the grains have He ages of <5 Ma (Campbell et al., 2005). This result appears to contradict the work of Zeitler (1985) who measured fission track apatite ages for 80 bedrock samples from a 350 km × 250 km area in the Nanga Parat region of the Indus basin and found that 90% of the apatites had implied exhumation rates <<1.0 km/Myr. The remaining 10% gave exhumation between 2.5 and 4.3 km/Myr, averaging 3.1 km/Myr. The obvious explanation for this apparent discrepancy is that regions with high exhumation rates are providing a disproportionate fraction of the Indus River load. Compression of isotherms in areas of high relief (Zeitler, 1985; Brewer et al., 2003) or adjacent to thrusts may contribute to the variability of the short-term exhumation rates.

5.3 Short-term exhumation rates higher than long-term exhumation rates

If we assume that rapid rock uplift is the primary cause of high short-term exhumation rates, the variability in the short-term exhumation rates imply that the vertical component of movement on faults is highly variable over the different parts of the Himalayas on a time scale of <5 Myr. This could be interpreted to indicate that uplift is spatially focused into a few regions where mid-crustal flow has pushed material into long-lived, rapidly exhuming aneurysms (Zeitler et al., 2001). However, the consistency of the long-term rates require the high rates of short-term crustal uplift to be transient: areas of rapid short-term uplift must become areas of slow uplift and areas of current slow short-term uplift must have had a previous history of rapid uplift in order to attain the long-term average. For example, six zircons that yield short-term exhumation rates between 2.32 and 2.67 km/Myr (Table 4), which are similar to the rates for the Central Crystallines of the Greater Himalayan, have probably come from that source. Their short-term rates exceed their long-term rates by 0.91–1.51 km/Myr showing that the rapid modern exhumation (uplift) of the Central Crystallines of the Greater Himalayan recorded by Vance et al. (2003) cannot have lasted more than ~15 Myr. Lavé and Avouac (2001) also considered that the sharp relief together with the high uplift rates in the Higher Himalaya reflects thrusting over the mid-crustal ramp rather than the isostatic response to re-incision of the Tibetan Plateau driven by the late Cenozoic climate change, or the late Miocene reactivation of the Main Central Thrust.

An alternative tectonic hypothesis is that the vertical vector of movement on the major faults that separate the various Himalayan terranes is transient with terranes that are currently undergoing rapid uplift having previous histories of slow uplift and *visa versa* on time scales of a few Myr (Zeitler, 1985; Copeland, 1997). However, this hypothesis fails to explain why the numbers of zircons with short-term exhumation rates that are greater than and less than the long-term rate are not sub-equal, unless rivers are biasing the detrital sample towards areas of rapid erosion as suggested earlier.

Vance et al. (2003) suggested movement of a thrust over a ramp that steepens by several degrees as it approaches the surface as the explanation for Himalayan short-term exhumation rates, calculated from fission track apatite ages, being generally higher than the long-term rates calculated from muscovite Ar ages. Major thrust faults must flatten with depth, and near surface steepening of thrusts is therefore likely to be a general feature of the convergent Himalayas. The vertical vector of a parcel of rock moving along such a thrust must increase as it approached the surface.

5.4 Long-term exhumation rates higher than short-term exhumation rates

Although the hypotheses discussed in the previous section may provide an explanation for the majority of the data showing short-term exhumation rates higher than long-term rates, they cannot explain the four samples for which the reverse is true. The zircons that have long-term exhumation rates exceeding their short-term rate have the slowest short-term rates (Table 4) and may come from an area that experienced rapid exhumation on the South Tibetan Fault

Zone prior to 17 Ma, as suggested by White et al. (2002). Their study of 12 to 21 Ma foreland basin sandstones from the Lower Siwalik and Dharamsalt Formations found a sudden change in lag time, the difference between the minimum Ar age of detrital muscovite grains and the sedimentation age, from 1–3 to ~10 Myr at 17 Ma. They argued that this change required a change in the exhumation rate of the Dharamsalt Formation source region from up to 5 to <1 km/Myr, which they attributed to a reduction in the rate of movement on the South Tibetan Fault Zone at 17 Ma.

Comparative studied of exhumation rates in small basins with simple geology, using both bedrock and double-dating detrital zircon methods, are required to distinguish between the various possibilities discussed in this paper.

6 Conclusion

The U-Pb-He double-dating method has been successfully used to determine short- and long-term exhumation rates from detrital zircons shed from the Himalayan Mountains. They show that the short-term rates are generally higher and more variable than the long-term rates although, for the zircons with the slowest short-term exhumation rates, the long-term rates are higher than the short-term rates. The advantage of the U-Pb-He double-dating method is that it allows the short- and long-term cooling and exhumation rates to be determined on the same detrital mineral, which is not possible by any other method. In addition, the U-Pb-He double-dating results for the detrital zircons from the Ganges river indicate that there was a protracted exposure of metamorphic rocks from deep crust to surface since the late episode of continental collision, and a prolonged overprint of amphibolite-facies metamorphism during the Himalaya orogeny.

This study was supported by the Australian Research Council Discovery Project (Grant No. DP 0556923), the Chinese Academy of Sciences Distinguished Professorship, and Guangzhou Institute of Geochemistry, Chinese Academy of Sciences (Grant No. Y234041001). We thank Prof. Yongfei Zheng for his constructive comments on the interpretation of age data.

Ahnert F. 1970. Functional relationships between denudation, relief and uplift in large mid-latitude drainage basins. Am J Sci, 268: 243–263

Beck R A, Sinha A, Burbank D W, et al. 1998. Climatic, oceanographic and isotopic consequences of the Paleocene India-Asia collision. In: Aubrey M P, Berggren W A, eds. Late Paleocene-Early Eocene Biotic and Climatic Events in the Marine and Terrestrial Record. IGCP Volume 308. Columbia: Columbia University Press. 103–117

Besse J, Courtillou V, Possi J P, et al. 1984. Paleomagnetic estimates of crustal shortening in the Himalayan thrusts and Zangbo suture. Nature, 311: 621–26

Brewer I D, Burbank D W, Hodges K V. 2003. Modeling detrital cooling-age population: Insights from two Himalayan catchments. Basin Res, 15: 305–320

Burbank D W, Blythe A E, Putkonen J, et al. 2003. Decoupling of erosion and precipitation in the Himalayas. Nature, 426: 652–655

Campbell I H, Reiners W, Allen C M, et al. 2005. He-Pb double dating of detrital zircons from the Ganges and Indus Rivers: Implication for quantifying sediment recycling and provenance studies. Earth Planet Sci Lett, 237: 402–432

Clift P D, Hodges K V, Heslop D, et al. 2008. Correlation of Himalayan exhumation rates and Asian monsoon intensity. Nat Geosci, 1: 875–880

Compston W, Williams I S, Meyer C. 1984. U-Pb geochronology of zircons from lunar breccia 73217 using a sensitive high mass-resolution ion micro-probe. J Geophys Res, 89(Suppl): 525–534

Copeland P, Harrison T M, Kidd W S F, et al. 1987. Rapid early Miocene acceleration of uplift in the Gangdese Belt, Xizang (southern Tibet), and its bearing on accommodation mechanisms of the India-Asia collision. Earth Planet Sci Lett, 86: 240–252

Copeland P. 1997. The when and where of the growth of the Himalaya and Tibetan Plateau. In: Ruddiman W, ed. Tectonics Uplift and Climate Change. New York: Plenum Publishing. 19–40

Farley K A, Wolf R A, Silver L T. 1996. The effects of long alpha-stopping distances on (U-Th)/He ages. Geochim Cosmochim Acta, 60: 4223–4229

Farley K A. 2007. He diffusion systematics in minerals: evidence from synthetic monazite and zircon structure phosphates. Geochim Cosmochim Acta, 71: 4015–4024

France-Lanord C, Derry L, Michard A. 1993. Evolution of the Himalaya since Miocene time—Isotopic and sedimentological evidence from the Bengal fan. Geol Soc Spec Publ, 74: 603–621

Hodges K V. 2000. Tectonics of the Himalaya and southern Tibet from two perspectives. Geol Soc Am Bul, 112: 324–350

Hourigan J K, Reiners P W, Brandon M T. 2005. U-Th zonation-dependent alpha-ejection in (U-Th)/He chronometry. Geochim Cosmochim Acta, 69: 3349–3365

Jain A K, Kumar D, Sigh S, et al. 2000. Timing, quantification and tectonic modelling of Pliocene-Quaternary movements in the NW Himalaya: Evidence from fission track dating. Earth Planet Sci Lett, 179: 437–451

Kaneko Y, Katayama I, Yamamoto H, et al. 2003. Timing of Himalayan ultrahigh-pressure metamorphism: sinking rate and subduction angle of the Indian continental crust beneath Asia. J Metamorph Geol, 21: 589–599

Lavé J, Avouac J P. 2001. Fluvial incision and tectonic uplift across the Himalayas of central Nepal. J Geophys Res, 106 (Bll): 26561–26591

Li W C, Chen R X, Zheng Y F, et al. 2013. Zirconological tracing of transition between aqueous fluid and hydrous melt in the crust: Constraints from pegmatite vein and host gneiss in the Sulu orogen. Lithos, 162-163: 157–174

Longerich H P, Jackson S E, Günther D. 1996. Laser ablation inductively coupled plasma mass spectrometric transient signal data acquisition and analyte concentration calculation. J Analy Atom Spect, 11: 899–904

Parrish R R, Gough S J, Searle M P, et al. 2006. Plate velocity exhumation of ultra-high pressure eclogites in the Pakistan Himalaya. Geology, 34: 989–992

Pearce N J G, Perkins W T, Westgate J A, et al. 1997. A compilation of new and published major and trace element data for NIST SRM 610 and NIST SRM 612 glass reference materials. Geostand Newsl, 21: 115–144

Rahl J, Reiners P W, Campbell I H, et al. 2003. Combined single grain (U-Th)/He and U/Pb dating of detrital zircons from the Navajo Sandstone, Utah. Geology, 31: 761–64

Reiners P W, Spell T L, Nicolescu S, et al. 2004. Zircon (U-Th)/He thermochronometry He diffusion and comparisons with $^{40}Ar/^{39}Ar$ dating. Geochim Cosmochim Acta, 68: 1857–1887

Reiners P W. 2005. Zircon (U-Th)/He thermochronometry. In: Reiners P W, Ehlers T A, eds. Thermochronology. Rev Mineral Geochem, 58: 151–176

Reiners P W, Brandon M T. 2006. Using thermochronology to understand orogenic erosion. Annu Rev Earth Planet Sci, 34: 419–466

Shuster D L, Flowers R M, Farley K A. 2006. The influence of natural radiation damage on helium diffusion kinetics in apatite. Earth Planet

Sci Lett, 249: 148–161
Stewart R J , Hallet B, Zeitler P K, et al. 2008. Brahmaputra sediment flux dominated by highly localized rapid erosion from the easternmost Himalaya. Geology, 36: 711–714
Tonarini S, Villa I, Oberli M, et al. 1993. Eocene age of eclogite metamorphism in Pakistan Himalaya: Implications for India-Eurasia collision. Terra Nova, 5: 13–20
Vance D, Bickle M, Ivy-Ochs S, et al. 2003. Erosion and exhumation in the Himalaya from cosmogenic isotope inventories of river sediments. Earth Planet Sci Lett, 206: 273–288
Watson E B, Harrison T M. 1983. Zircon saturation revisited-temperature and composition effects in a variety of crustal magma types. Earth Planet Sci Lett, 64: 295–304
Watson E B, Harrison T M. 2005. Zircon thermometer reveals minimum melting conditions on earliest earth. Science, 308: 841–844
White N M, Pringle M, Garzanti E, et al. 2002. Constraints on the exhumation and erosion of the High Himalayan Slab, NW India, from foreland basin deposits. Earth Planet Sci Lett, 195: 29–44
Williams I S. 2001. Response of detrital zircon and monazite, and their U-Pb isotopic systems, to regional metamorphism and host-rock partial melting, Cooma Complex, southeastern Australia. Aus J Earth Sci, 48: 557–580
Yin A. 2006. Cenozoic tectonic evolution of the Himalayan orogen as constrained by along-strike variation of structural geometry, exhumation history, and foreland sedimentation. Earth Sci Rev, 76: 1–131
Yin A, Harrison T M. 2000. Geologic evolution of the Himalayan-Tibetan orogen. Annu Rev Earth Planet Sci, 28: 211–280
Zeitler P K. 1985. Cooling history of the NW Himalaya, Pakistan. Tectonics, 4: 127–151
Zeitler P K, Koons P O, Bishop M P, et al. 2001. Crustal reworking at Nanga Parbat, Pakistan: Metamorphic consequences of thermal-mechanical coupling facilitated by erosion. Tectonics, 20: 712–728
Zheng Y F. 2009. Fluid regime in continental subduction zones: Petrological insights from ultrahigh-pressure metamorphic rocks. J Geol Soc Lond, 166: 763–782
Zheng Y F. 2012. Metamorphic chemical geodynamics in continental subduction zones. Chem Geol, 328: 5–48
Zheng Y F, Zhao Z F, Chen Y X. 2013. Continental subduction channel processes: Plate interface interaction during continental collision. Chin Sci Bull, 58: 4371–4377
Zhu B, Kidd W S F, Rowley D B, et al. 2005. Age of Initiation of the India-Asia Collision in the East-Central Himalaya. J Geol, 113: 265–285